Hindawi
International Journal of Antennas and Propagation
Volume 2022, Article ID 8157541, 14 pages
https://doi.org/10.1155/2022/8157541

Research Article

Design of Crossed Dipole Yagi–Uda MIMO Antenna for Radar Applications

K. Malaisamy,[1] **G. Haridoss**,[2] **J. Arun Pandian**,[3] **and Samira Kabir Rima**[4]

[1]*Department of Electronics and Communication Engineering, Saranathan College of Engineering, Tiruchirappalli, India*
[2]*Department of Electronics and Communication Engineering, M.A.M College of Engineering and Technology, Tiruchirappalli, India*
[3]*School of Information Technology and Engineering, Vellore Institute of Technology, Vellore, India*
[4]*Department of Computer Science and Engineering, American International University, Dhaka, Bangladesh*

Correspondence should be addressed to Samira Kabir Rima; samirakabirrima@gmail.com

Received 8 October 2022; Revised 19 November 2022; Accepted 21 November 2022; Published 6 December 2022

Academic Editor: Trushit Upadhyaya

This work proposes, builds, and manufactures a small, high-gain MIMO antenna for radar applications. Using a Parasitic elements such as director & reflector show a simple method for increasing the gain and bandwidth of a Yagi-Uda Antenna. Using a Parasitic elements such as director and reflector show a simple method for increasing the gain and bandwidth of a Yagi-Uda Antenna. Using a nearby parasitic director and reflector. Also, it shows a simple method for increasing the gain and bandwidth of a Yagi–Uda antenna. A strip with a parasitic director is placed close to the top dipole element to improve the gain as well as bandwidth attributes of the Yagi–Uda antenna. The antenna performance parameters are investigated for 1×2 MIMO, cross dipole MIMO antenna (1×4), and an array configuration (two 1×4). It has high gain and operates in the *S*-band (2 GHz–4 GHz). This antenna supports three bands and has a highest maximum directive gain of 12.5 dBi at 2.5 GHz and a bandwidth of 0.21 GHz. It is made of FR4 substrate. The suggested structure is 120 mm × 70 mm in size. Due to its high gain and less return loss, this antenna is better suited to radar applications.

1. Introduction

An antenna is a device that converts electrical power into radio waves and the other way around. An antenna is essential in wireless communications. MIMO (multiple input multiple output) is a wireless antenna system in which many antennas are used at the transmission and reception. In comparison to conventional radar, MIMO radar allows for simultaneous transmission and reception by utilizing multiple antennas. The SISO channel's performance is insufficient, and fading will have a greater impact on the system than a MIMO antenna. The addition of some arms to the basic dipole element enhances the bandwidth while improving the gain [1]. Because of its simple structure, improved bandwidth, and stable gain, a series-fed two-dipole antenna array was used in the base station antenna elements. Series-fed dipole pairs can produce broadband and dual-band characteristics. By changing the dimension of the dipole elements, the operating frequency could be varied, and the return loss could be controlled by varying the separation between the dipole elements [2]. The use of a parasitic strip pair director to enhance the bandwidth of a series-fed dipole pair (SDP) antenna is described [3]. A wideband planar Yagi–Uda antenna suitable for MIMO system design is presented, with working frequencies in the range from 1.8 GHz to 3.5 GHz [4].

For satellite application, a variety of antennas are designed using various techniques. A compact 4×4 MIMO antenna for UWB applications is built on a Rogers RT5870 substrate, but it has a low gain of 3 dBi [6]. A dual-band WLAN/UWB broad slot microstrip-fed antenna with FR4 substrate with reduced mutual coupling, reduced envelope correlation, and radiation efficiency of 85–95% is developed [7, 8]. A simple, small dual-polarized UWB MIMO antenna for Wi-MAX and WLAN systems is presented. A tiny MIMO antenna for WLAN, Wi-MAX, and UWB

applications is given. The ramped ground stub protrudes vertically to increase isolation [9, 10].

A MIMO band-notched antenna with a small footprint of $22 \times 36\,\text{mm}^2$ is presented. Two meander lines, a connection line, and a short parasitic line are used to improve isolation between the two input ports. In order to create the band-notched characteristics, an open stub in the radiator was used. The antenna structure was somewhat difficult and needed more fabrication accuracy [11]. The antenna operates in the ISM band and has a center frequency of 2.45 GHz. There are eight Yagi–Uda antennas arranged in a circle. Each Yagi_Uda antenna consists of a bent reflector, abent driven and a bent director. PIN diodes [12] share the bent reflector for different Yagi–Uda antennas. For indoor applications, a dense packed coplanar waveguide (CPW)-fed MIMO antenna was developed. The antenna is $31 \times 43\,\text{mm}^2$ in size. The antenna covers a frequency range of 3.9 to 8.1 GHz. The mutual coupling between the antennas was less than −15 dB for practically the whole bandwidth, peaking at −31 dB at 5.4 GHz [13]. A wideband four-port MIMO antenna [25], flexible four-port MIMO antenna [26], and four-port ground-coupled MIMO antennas [27] were designed.

According to the literature review, the isolation, gain, and return loss are all low. The array MIMO antenna has a large size. To address the aforementioned concerns, a MIMO antenna using a cross dipole array MIMO antenna is developed in this attempt. The existing antennacharacteristics including Bandwidth and directivity are less. Several initiatives have been taken to realize the structure for *S*-band and UWB operations, where the array elements are joined serially or parallelly. As a solution, the cross dipole has been researched as an exhibit component in 1×2, 1×4, and two 1×4 MIMO cluster topologies. Different cluster structures have exhibited high directivity and an upgraded signal-to-noise proportion.

This paper describes a revolutionary small size crossed dipole Yagi–Uda MIMO microstrip patch antenna for *S*-band radar applications. A cross dipole is utilized related to a balun to accomplish high gain and adjusted feed activity. The balun is introduced and it matches the input impedance of a radio wire to the 50 Ω feed line [5]. To increase overall gain, a crossed dipole Yagi–Uda MIMO antenna (1×4) and an array arrangement (two 1×4) were studied for 1×2 MIMO. It is suited for radar communication because of its high gain, compact size, and balanced operation.

The rest of the paper is organized as follows. Section 2 describes the structure and design technique for the microstrip patch antenna. Section 3 shows how to build the crossed dipole Yagi–Uda MIMO antenna in detail. Section 4 explains the patch's array implementation, followed by Section 5 which is devoted to the study of the measurements and the simulated results. Section 6 brings the paper to a close.

2. Construction of Antenna

On a FR4 substrate, the antenna presented here is 120 mm 70 mm in dimensions. Table 1 displays the antenna parameters and data. The antenna's structural parameter values are as follows. The patch's length (L) is 70 mm, and its width (W) is 120 mm. $W3 = 35$ mm between the ground plane and the first dipole ($D2$), and $W2 = 35$ mm between the first dipole ($D2$) and the next dipole ($D1$). $W4 = 20$ mm ground plane height, and $L2 = 20$ mm for the width of the coplanar strip line (W_{CPL}). The substrate's height (H) is 1.6 mm, and the balun's length (W_F) is 40 mm. The director's length and width are $W0$ and $W1$, respectively.

As illustrated in Figure 1, this antenna is made up of four dipole antennas that are crossed to produce a cross dipole Yagi–Uda MIMO antenna. The size is scaled up by 0.8 to function at a lower operating frequency. FR4 is used due to its inexpensive raw material prices, simplicity of fabrication, and ability to give great performance in a broad range of purposes [14]. Table 2 describes the design specifications.

3. Design Procedure

3.1. Design of a Single Element Antenna. A new structure has been proposed to improve the operation of the antenna in the existing system. A novel construction is implemented and adjusted to build a single element antenna in order to obtain a high gain and efficiency. A single antenna is made up of multiple parallel elements in a line with two parts: Driven and Parasitic. l. The reflector element of the antenna is slightly longer than the driven dipole element, and the directors are slightly shorter as shown in Figure 2. When compared to a conventional antenna, this type of design provides a higher antenna gain, bandwidth, and efficiency. On a FR4 substrate (dielectric constant = 4.4, $\tan\delta = 0.02$), the proposed antenna is printed. Its operating frequency is 2.45 GHz. The structure's feed line is fixed at the bottom of the patch, and a 50 Ω feed line is to be provided. The proposed antenna was designed; simulation of the antenna was performed using CST Studio Suite (simulation tool).

3.2. Design of Balun. A balun is required for the feeding mechanism needed to restore balance to an unbalanced transmission line. The balun is constructed in such a way that its input impedance equals 50 Ω, allowing the intended antenna to be supplied through the hole. An incorporated balun is constructed between the microstrip (MS) and CPS lines to match the antenna's input impedance with a range of 50 Ω feed lines. The feed position is used to short the end of the MS line with a shorting pin. $L2$ represents the breadth of the CPS line.

3.3. Design of MIMO Antenna (1×2). To make (1×2) MIMO, the two antennas are placed in series manner as shown in Figure 3.

3.4. Cross Dipole MIMO Antenna Design (1×4). A cross dipole Yagi–Uda MIMO antenna is suggested to improve the gain and bandwidth of a series-fed two-dipole antenna (STDA). Antennas 1 and 2 are designed in series, followed by antennas 3 and 4. The antenna's two pairs are cross-coupled to each other. Figures 4(a) and 4(b) show the top cut first pair of antennas and the top cut second pair of antennas. It converges

Table 1: Single dipole element design parameters.

Specification	Values (mm)
W	120
L	70
$W0$	8
$W1$	10
$W2$	35
$W3$	35
$W4$	20
$L1$	25
$L2$	20
L_f	4
W_c	85
W_f	40

each other to create the cross dipole MIMO antenna; as delineated in Figure 1, the general aspect is brought down in this work by joining the double elements to frame a cross dipole antenna. At the center, a pair of antennas is joined. When we cross-coupledthe antennas, it occupied a little space. MIMO antenna is installed on FR4 substrate. It uses four cross-coupled antennas to operate at different resonant frequencies. The four antennas have the same dimensions. The cross dipole antenna is made up of eight dipole elements that are same but phase opposite. The balun supplies two ports to each single dipole element. When formed into a cross dipole, this type of structure takes up less space.

The design steps of 1×4 MIMO antenna are illustrated in Figure 5. The first step in designing a single element is to design two circular patch dipoles with different lengths and a ground plane. The second step is to design a balun for balance and an unbalanced transmission line. The circular patches are connected to the coplanar strip (CPS) line using smooth shape progress. A pair of parasitic directors is appended above the radiating element to improve the gain, return loss, and bandwidth of antenna. In step 3, a two-element MIMO antenna is formed. The two-element MIMO antenna operates at two frequencies: 1.8 GHz and 2.45 GHz. Step 4 depicts the assembly of 1×4 MIMO antennas with dual frequencies of 2.18 GHz and 2.52 GHz in the S-band. When the two antennas are cross shaped, the 1×4 MIMO antenna takes up less space. It provides high gain.

3.5. Fabrication. Figure 6 depicts a photograph of a constructed cross dipole Yagi–Uda MIMO antenna. Figure 4(b) depicts the front view of the constructed MIMO antenna with a single top cut element, whereas Figure 4(a) shows the rear view of the constructed MIMO antenna with a single top cut element. The antenna's entire size is approximately $120\ \text{mm} \times 70\ \text{mm} = 8400\ \text{mm}^2$.

4. Formation of Array

The Two (1×4) MIMO array is depicted in Figure 7. The distance between the two elements is 36 mm, as calculated by equation $W/2$ [15]. It consists of eight components and eight ports, which are labelled as S_{11}, S_{22}, $S_{33,}$ . . ., and S_{88}, S_{11} for input port voltage reflection, S_{22} for output port voltage reflection, S_{21} for forward voltage gain, and S_{12} for reverse voltage gain. The input-output relationships between the ports are described by the scattered parameters.

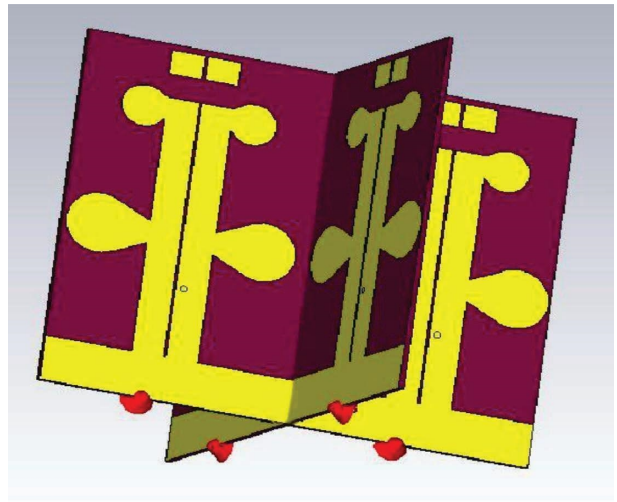

Figure 1: The suggested cross dipole MIMO antenna model.

Table 2: Specification of single element antenna.

Sl. no.	Specification	Value
1	Dielectric constant (ε_r)	4.4
2	Substrate height (h)	1.6 mm
3	Loss tangent (tanδ)	0.02
4	Patch length	120 mm
5	Patch width	70 mm
6	Thickness	1.6 mm

5. Results and Discussion

5.1. The Single Antenna's Return Loss (S_{11}), Gain, and Directivity. Figure 8 shows a graph of the single antenna's simulated and observed return loss (S_{11}). At 2.5 GHz, the return loss of a single antenna is −33.85 dB. Figure 9 displays the 1×2 MIMO design's simulated and measured S parameter (S_{11}) findings. As demonstrated in Figure 9, the antenna has achieved broadband impedance matching in the S-band frequency range. The greatest return loss was around −45 dB. A dual resonance in the S-band was produced and calculated, as expected.

The simulated and measured results of the S parameter (S_{11}) for the developed 1×4 MIMO antenna design are shown in Figure 10. This MIMO antenna has a return loss of −30 dB at 2.1 GHz and −44 dB at 2.5 GHz. It has dual-band capability. The simulation results of the S parameter (S_{11}) for the developed the two (1×4) MIMO antenna design are depicted in Figure11. This MIMO antenna has a return loss of −30 dB at 2.1 GHz and −44 dB at 2.5 GHz. It has dual-band capability.

5.2. Parametric Analysis. A parametric analysis is carried out to demonstrate the fine adjustment of the proposed antenna's port isolation and S parameters. The simulated S parameters of port 1 for varying the length of dipole 2 ($L4$)

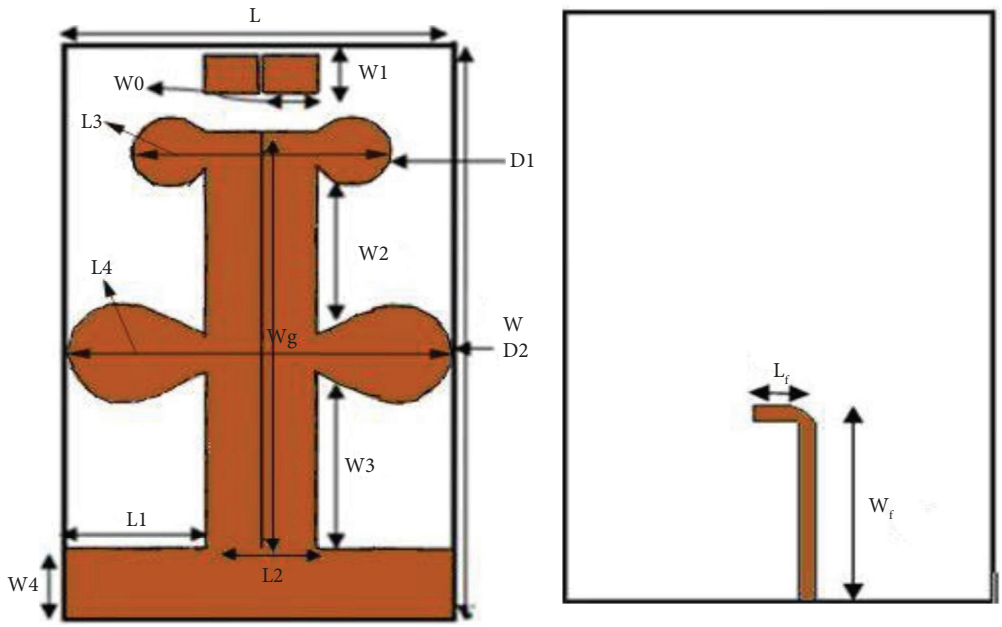

Figure 2: A single element antenna is shown schematically: (a) front and (b) back views.

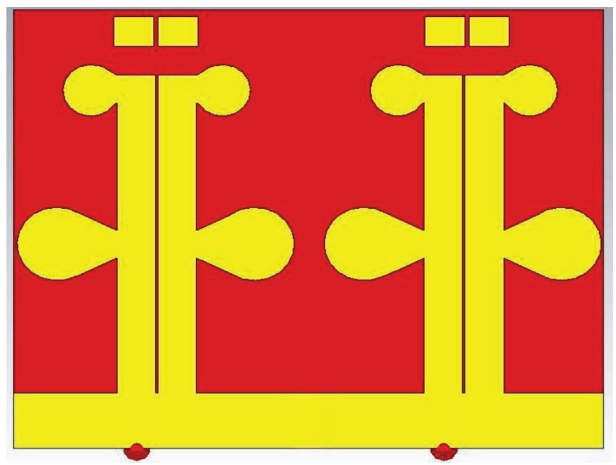

Figure 3: Schematic representation of 1×2 MIMO antenna.

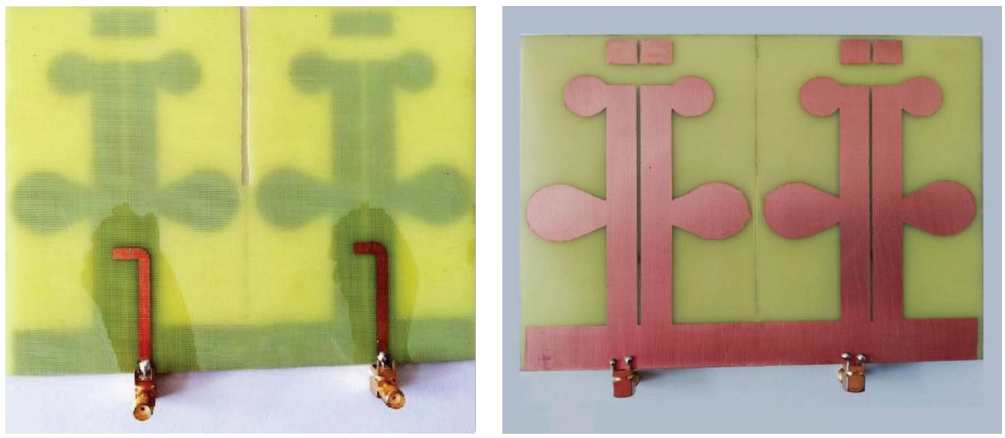

Figure 4: Fabricated 1×2 MIMO antenna with top cut: (a) back view; (b) front view.

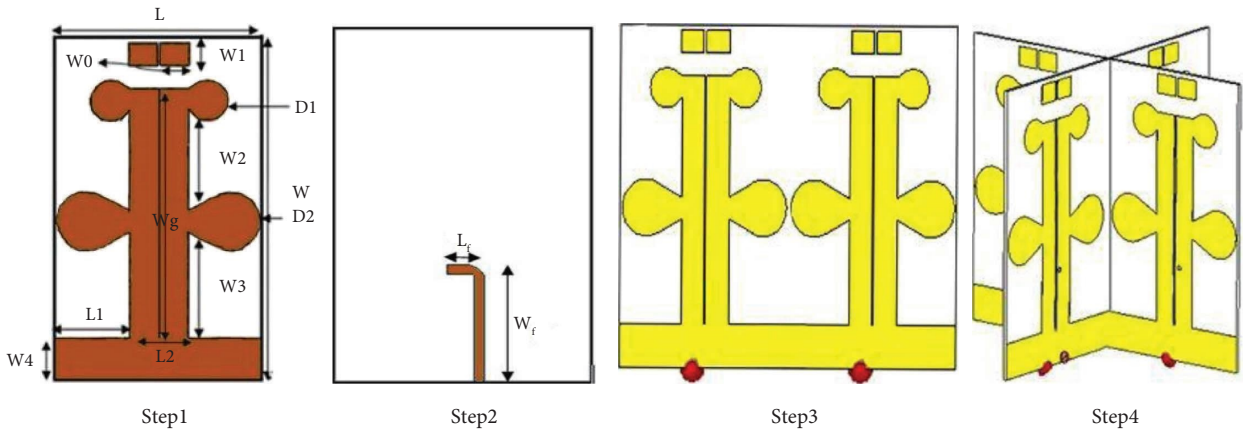

Figure 5: Design steps of the four-port MIMO antenna.

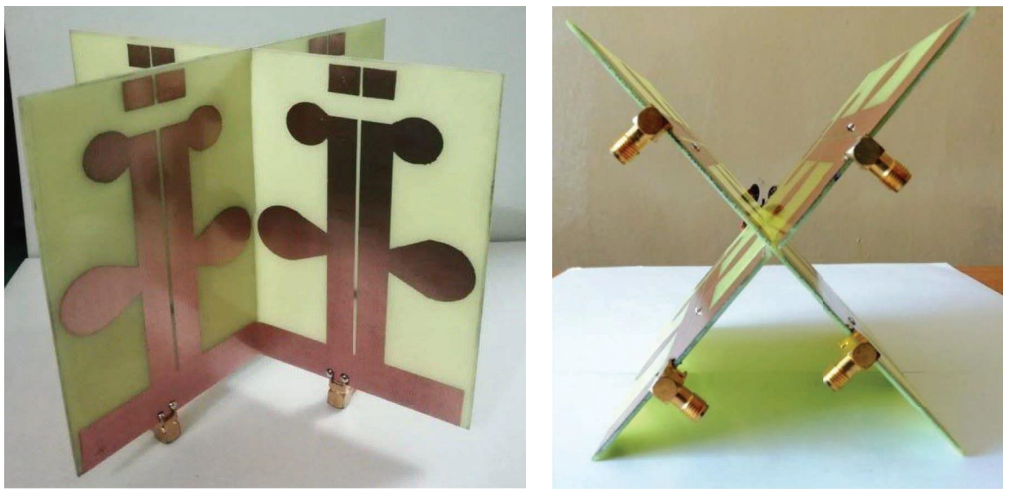

(a) (b)

Figure 6: (a) Front view of the manufactured cross dipole Yagi–Uda MIMO antenna. (b) Side view.

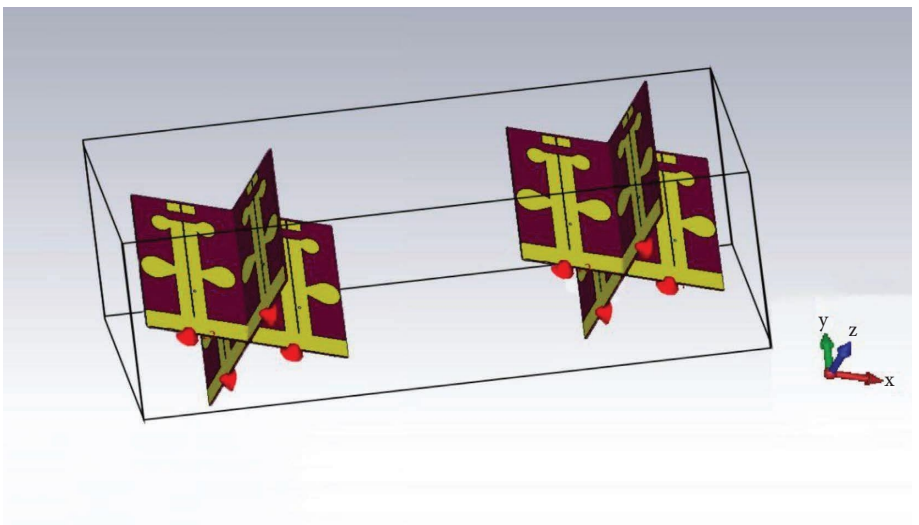

Figure 7: Model of the two (1 × 4) MIMO array set up.

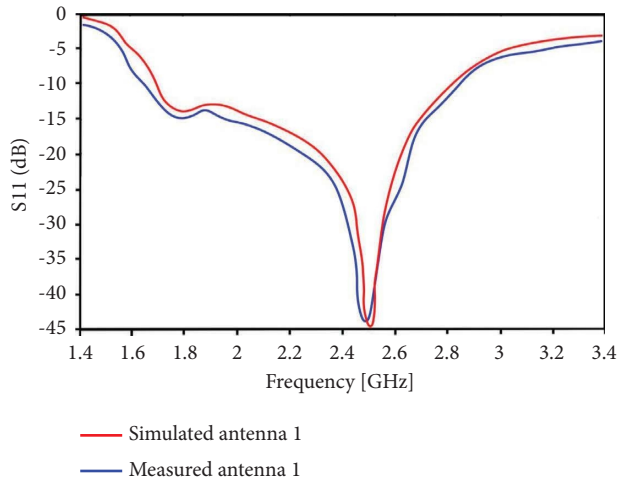

Figure 8: The single antenna's return loss performance.

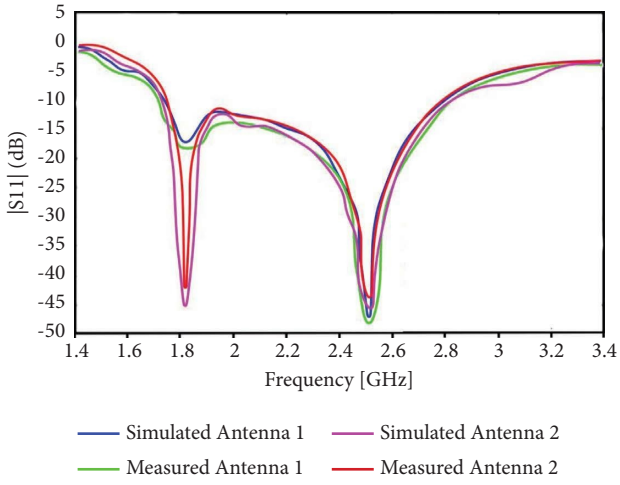

Figure 9: 1 × 2 MIMO antenna's return loss.

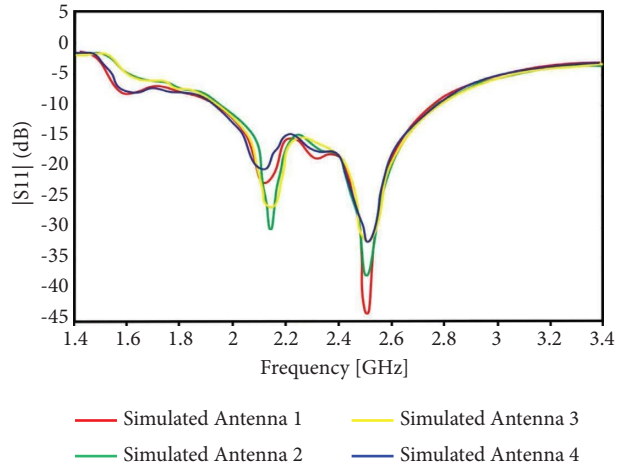

Figure 10: 1 × 4 MIMO antenna's return loss.

are shown in Figure 12. $L4$ results ranging from 62 mm to 66 mm are presented. Figure 12(a) shows very minor effects on S_{11}. The antenna's low band shifts to lower frequencies as the length of dipole 2 increases for S_{12} of two adjacent ports shown in Figure 12(b). S_{13} in Figure 12(c) exhibits better isolation.

The simulated S parameters of port 1 for varying the length of dipole 1 ($L3$) are shown in Figure 13. The results for $L3$ ranged from 32 mm to 36 mm. Figure 13(a) shows very minor effects on S_{11}. The antenna's high band is shifted to higher frequencies as the length of the dipole 1 increases for S_{12} of two adjacent ports shown in Figure 13(b). S_{13} in Figure 13(c) exhibits better isolation.

5.3. Radiation Pattern. Figures 14(a)–14(d) depict the three-dimensional radiation pattern of a single antenna and 1 × 2, 1 × 4, and two 1 × 4 MIMO antennas. The simulated gain values of all antennas are displayed. The proposed antenna has a gain of 6.37 dBi for a single antenna, 9.32 dBi for (1 × 2) MIMO, 9.22 dBi for (1 × 4) MIMO and 12 dBi for two (1 × 4) MIMO antennas.

5.4. Gain. The proposed antenna emanates omnidirectional radiation and works in the S-band. Thus, the radiations are communicated and recuperated without misfortune in each open region, demonstrating that the radiation design gathered from the suggested MIMO antenna is the amount of the relative multitude of examples made by each exhibit part Figure 15 shows the simulated and measured radiation pattern of the single antenna at 2.4 GHz with the gain of 6.37 dBi which is being matched to the simulated pattern. Figure 16 shows the recreated and genuine radiation example of the 1 × 2 MIMO antenna with an increase of 9.32 dBi at 2.4 GHz.

5.5. Outcomes and Examination of the MIMO in Arrays. The proposed antenna beats traditional S-band radio wires regarding gain and input reflection coefficient (S_{11}). The proposed antenna shows an improved performance in terms of return loss, gain over the existing antennas in an S-band. The comparison of gain and return loss between the proposed single antenna and MIMO array antennas are analysed. It is observed that there is a great variation in the

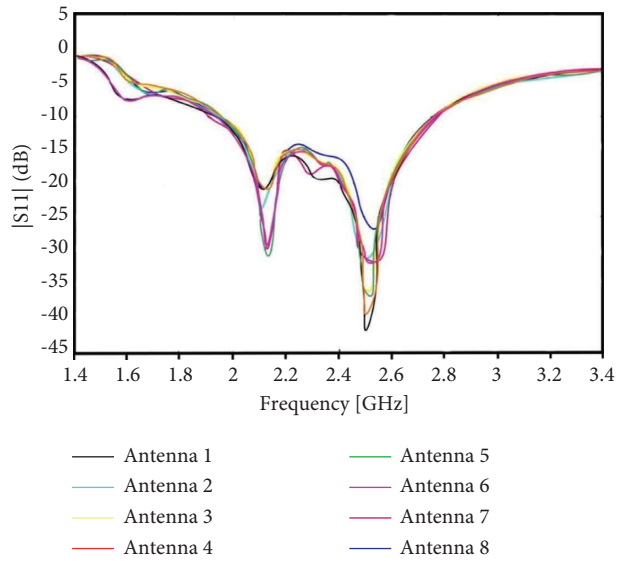

Figure 11: Return loss for two (1 × 4) MIMO antenna.

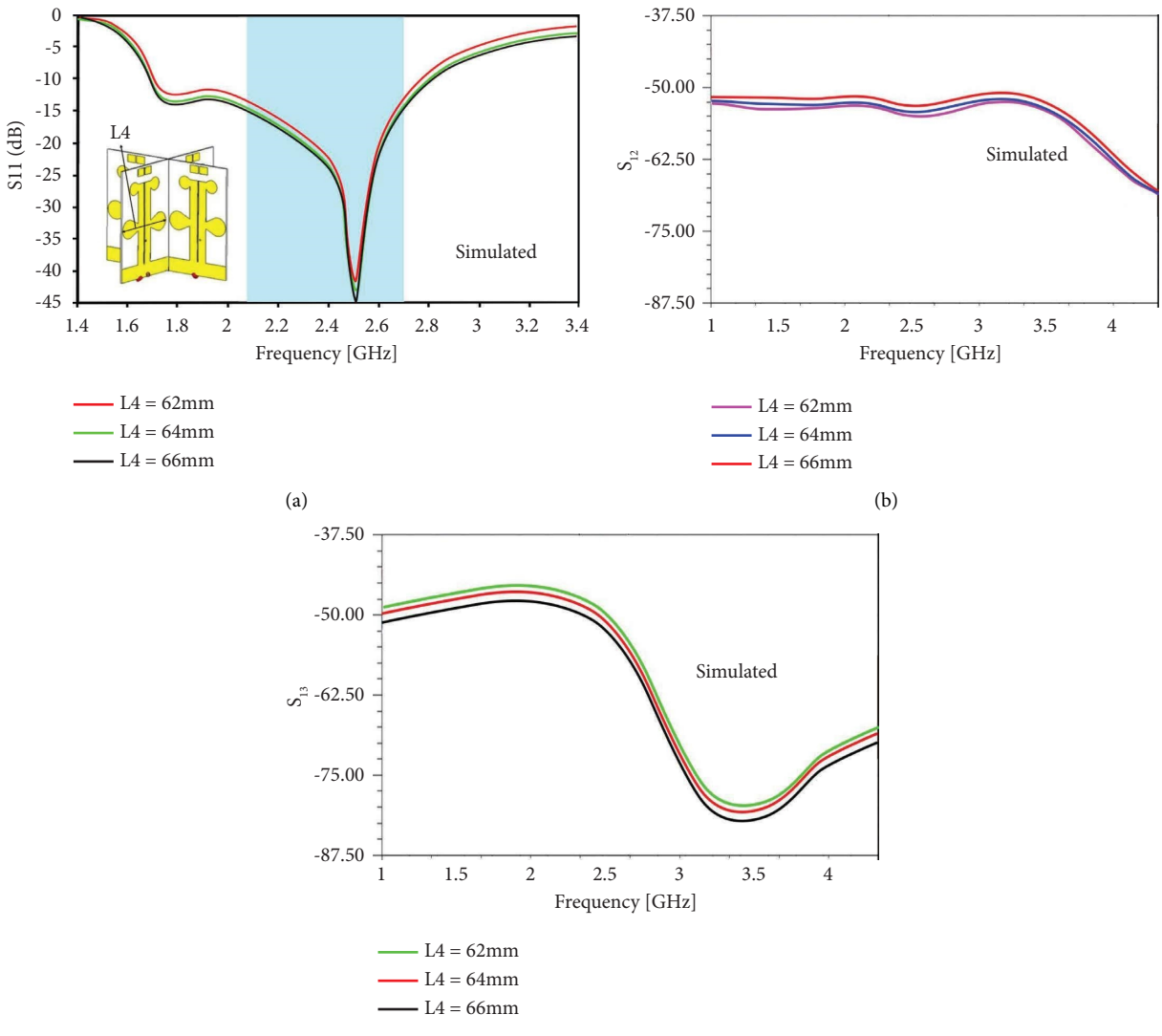

Figure 12: Simulated S parameters of port 1 for varying the length of dipole 2 ($L4$). (a) S_{11}. (b) S_{12}. (c) S_{13}.

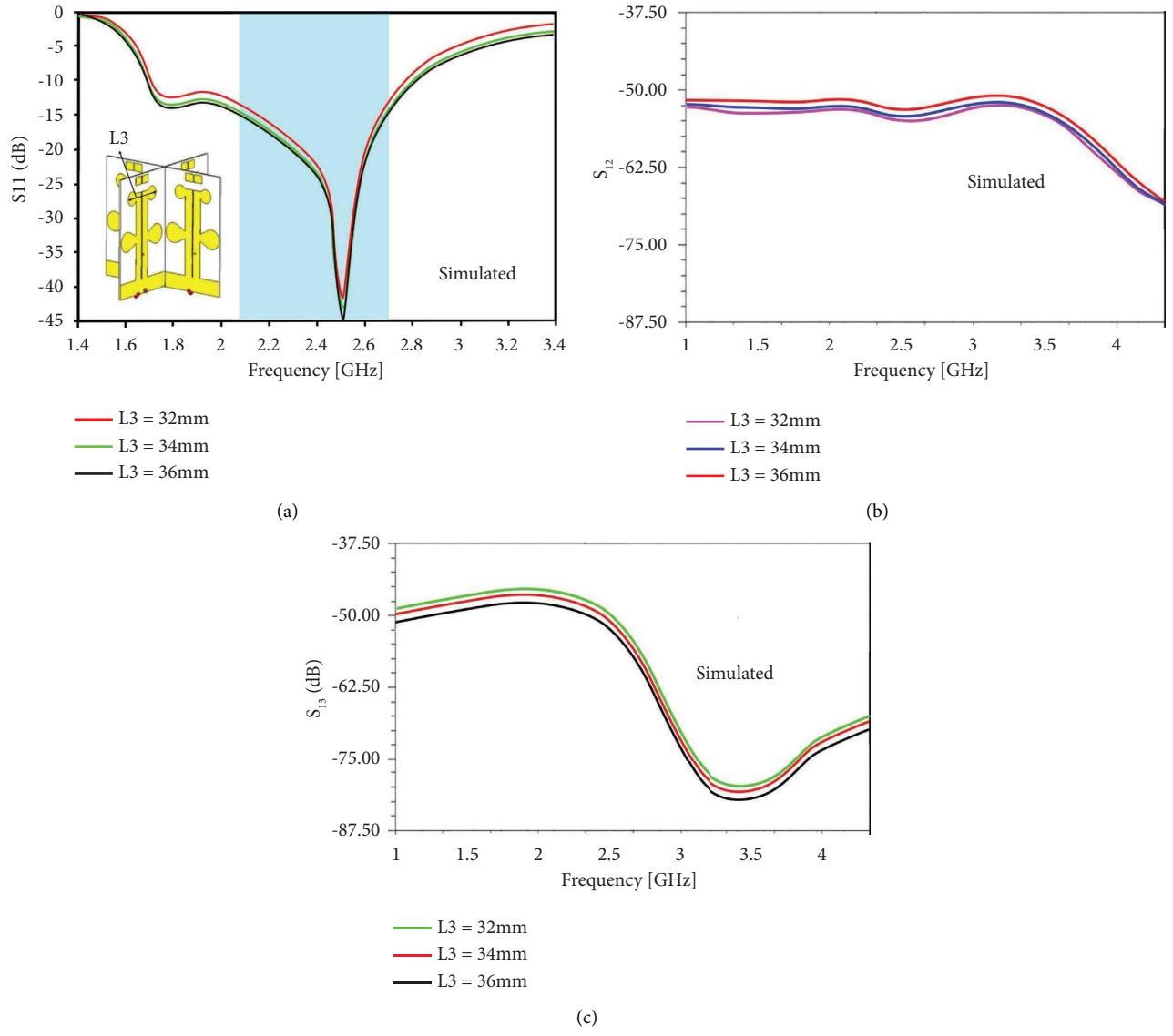

Figure 13: Simulated S parameters of port 1 for various length of dipole 1 ($L3$). (a) S_{11}. (b) S_{12}. (c) S_{13}.

antenna parameters between the single antenna and the formed array antennas. The performance of the antenna is significantly improved while there is an increase in the number of array elements, even at the cost of an increasing in size and complexity. The gain increases linearly when the radiating elements in the antenna are increased. The proposed antenna provides an efficient output by radiating each element By emanating every component, the proposed antenna produces an effective result.

5.6. Radiation Patterns of the Proposed Four-Port MIMO Antenna Array. Figure 17 depicts the measured and simulated radiation pattern in the E and H planes. The 2D patterns in the H plane are similar between antennas 1-2 and 3-4, whereas the E plane patterns are 180 degrees out of phase. Similarly, the antenna's E plane patterns are similar. The H plane patterns are 180 degrees out of phase with antennas 1-4 and 2-3. This demonstrates that the proposed antenna has achieved pattern diversity, ensuring no interference during reception and maintaining an omnidirectional radiation pattern in both the E plane and the H plane. It is also noted that the deviation between the simulated and measured results is very small, and any discrepancies may be due to fabrication inaccuracies or unavoidable conductor losses in the cable used during measurement analysis.

5.7. Gain and Efficiency of the Proposed Four-Port MIMO Antenna Array. Figure 18 depicts the proposed four-port MIMO antenna array's gain and efficiency. Because the other three antenna elements (antenna 2 to antenna 4) have identical structures, the gain and efficiency of antenna 1 are only measured here. The gain and efficiency results of antenna 1 measured from the proposed four-port MIMO antenna array are better than those of the two-port MIMO

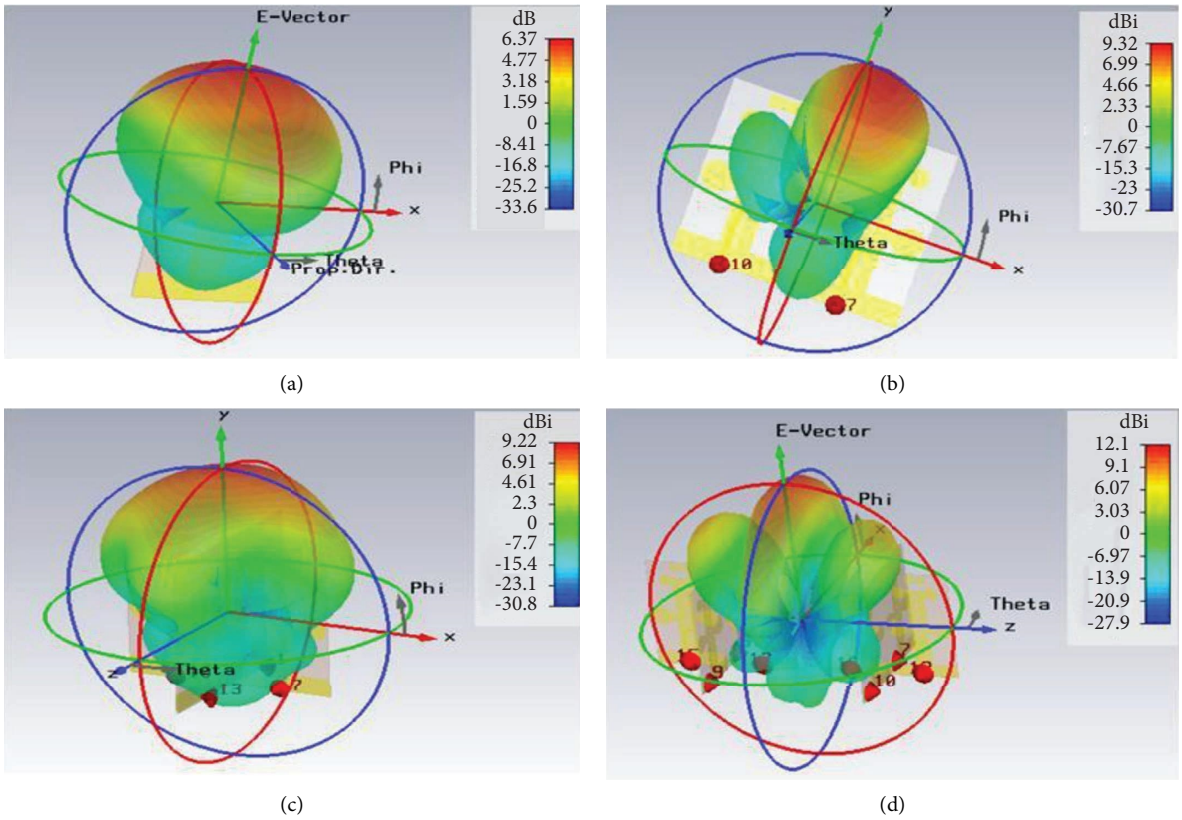

Figure 14: The 3D radiation pattern of (a) single antenna (b) 1 × 2 MIMO (c) 1 × 4 MIMO and (d) two antenna.

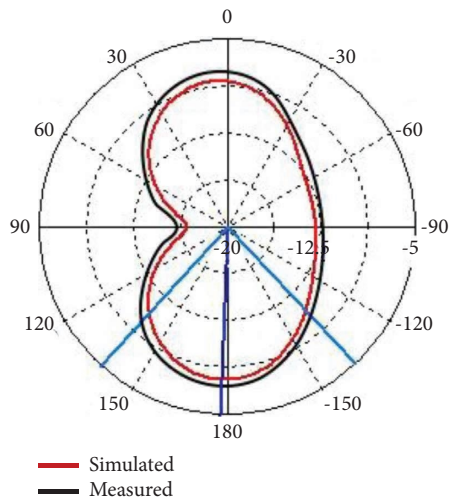

Figure 15: The single antenna's radiation pattern.

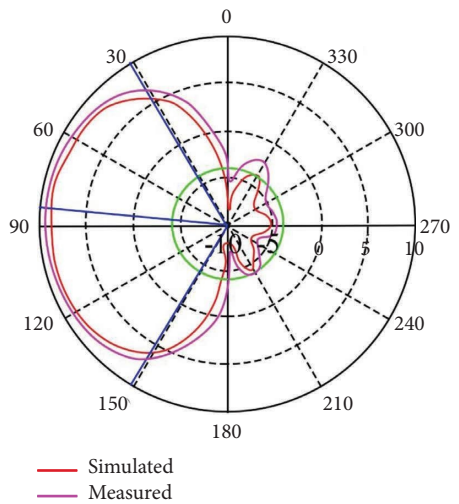

Figure 16: The radiation pattern of the 1 × 2 MIMO antenna.

antenna array, as shown in this figure. The measured gain and efficiency are well above 9.22 dBi and 87%, respectively.

5.8. Gain and Return Loss Examination for Various Cluster Setups. The gain of a single antenna, 1 × 2 MIMO, 1 × 4 MIMO, and two 1 × 4 MIMO array antennas for *S*-band applications is dissected and looked at. The proposed antenna beats existing *S*-band antenna in terms of return loss and gain.

From Table 3, analyzes the proposed antenna to exhibit array antennas. From the Table 3, it is noticed that there is a significant variation in the antenna parameters between the single antenna and the differently formed array antennas with various MIMO configurations. The performance of the antenna always improves with an increase in the number array elements, though it leads to an increase in size and complexity. VSWR is less than 2 for all the antennas.

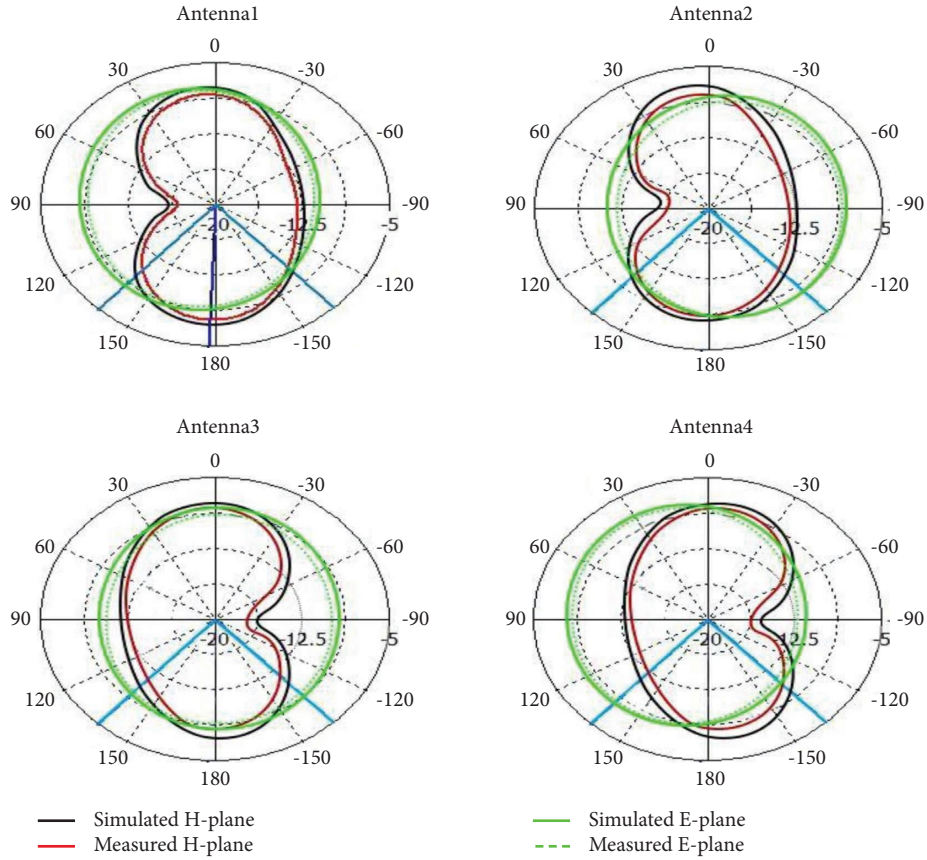

Figure 17: Simulated and measured radiation patterns in E plane and H plane.

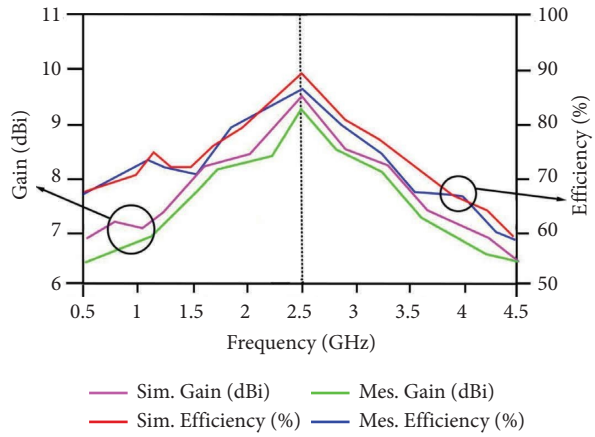

Figure 18: Simulated and measured gain and efficiency of the proposed four-port MIMO antenna array.

Table 3: Comparison of return loss (S_{11}), gain, and VSWR of projected antennas with different configuration.

S. no.	Types	S_{11} (dB)	Gain (dBi)	VSWR
1	Single	−45	6.37	1.1
2	1 × 2	−45	9.38	1.1
3	1 × 4	−45	9.38	1.1
4	Two 1 × 4	−45	12.1	1.1

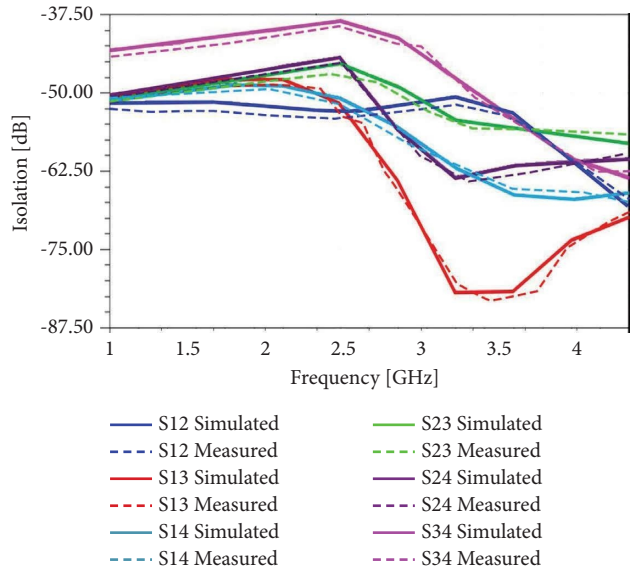

Figure 19: Simulated and measured isolation response of 1×4 MIMO antenna.

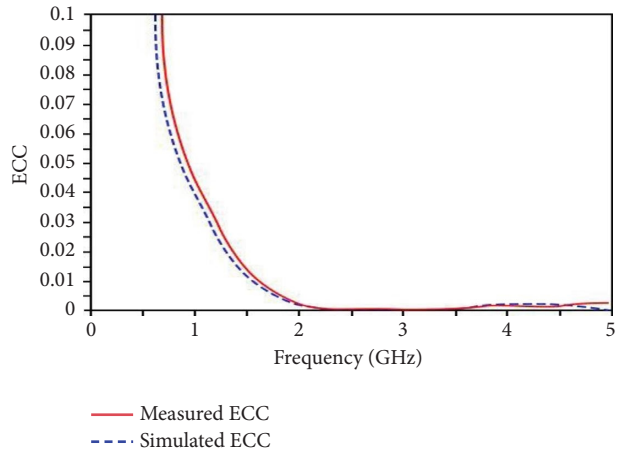

Figure 20: Simulated ECC response of 1×4 MIMO antenna.

5.9. Isolation. It utilizes the design of the type of antenna components to ascertain how much power is connected among neighboring antenna components. The simulated and measured isolation graph of the presented four-component MIMO antenna is displayed in Figure 19. The isolation between ports 1 and is not completely resolved, nor is the isolation between ports 1 and 3, ports 1 and 4, ports 2 and 3, and ports 3 and 2.

5.10. Envelope Correlation Coefficient. It is used to assess the feasibility of the suggested MIMO antenna. A low ECC necessitates the use of a MIMO antenna. The correlation between the branch signals acquired by the various elements is computed by ECC, and a lower ECC implies higher pattern variety [24]. The ECC between i and j is calculated using the following equation, assuming that the designed antenna is a lossless antenna in an isotropic scattering environment. The measured and simulated ECC values are given in Figure 20.

$$\rho_{eij} = \frac{\left|s_{ii}^{*}s_{ij} + s_{ji}^{*}s_{jj}\right|}{\left(1 - \left|s_{ii}\right|^{2} - \left|s_{ij}\right|^{2}\right)\left(1 - \left|s_{jj}\right|^{2} - \left|s_{ji}\right|^{2}\right)}. \quad (1)$$

Between port 1 and port 2, port 1 and port 3, port 1 and port 4, port 2 and port 3, port 2 and port 4, and port 3 and port 4, the EEC is calculated. The ECC of 1×4 structure is less than 0.0001.

5.11. Diversity Gain (DG) of the Proposed Four-Port MIMO Antenna Array. The calculated DG values from the S parameters and far-field patterns are shown in Figure 21. The DG values are observed to be greater than 9.22 dB. This ensures that the proposed four-port MIMO antenna array has good diversity performance.

5.12. Total Active Reflection Coefficient (TARC). The TARC is a parameter used to validate a MIMO antenna's performance in a single attempt. TARC is the ratio of total incident

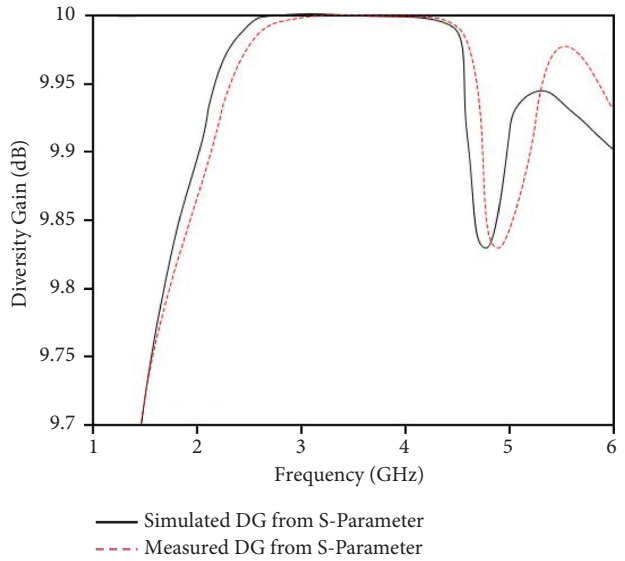

Figure 21: Diversity gain (DG) of the proposed four-port MIMO antenna array.

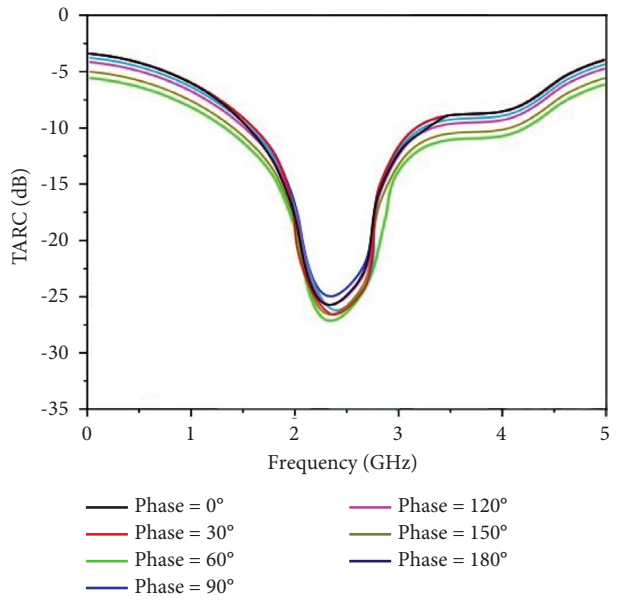

Figure 22: TARC curves of the proposed four-port MIMO antenna array.

Table 4: Comparison of the proposed MIMO antenna with reported antenna.

Ref.	No of antennas	Size	Return loss (dB)	Isolation (dB)	Frequency (GHz)	Bandwidth (MHz)	Gain (dB)	Efficiency (%)	ECC
[16]	4	$82.75 \times 54.82\ mm^2$	<−32	—	5.8	200	5.3	78.4	<0.0001
[17]	4	$120 \times 60\ mm^2$	—	>12	1.3–2.6	45 & 65	—	—	<0.2
[18]	4	$42.83 \times 34.48\ mm^2$	−28.75	>45	5.8	150	2	—	<0.0001
[19]	4	$60 \times 60\ mm^2$	−19	>19	3.4–3.8	400	4.5	—	<0.12
[20]	4	$130 \times 90\ mm^2$	−18	10	0.6, 1, 6	700	6.9	70	≤0.50
[21]	4	$40 \times 25\ mm^2$	—	5.5	2.2–2.45	180	6.55	75 & 85	0.175
[22]	4	$12 \times 12\ mm^2$	−22	—	36	—	10.6	80	—
[23]	4	$39 \times 39\ mm^2$	−22	>22	3.25–3.75 5.08–5.90	2.3–13.75	1.4–4.6	—	<0.02
This work	4	$120\ mm \times 70\ mm^2$	−45	>55	1.8–2.5	700	12.1	87.5	0.0001

power to total radiated power of a MIMO antenna array. The measured TARC values are shown in Figure 22. The TARC values are nearly constant across the operating bands, indicating that the proposed MIMO antenna system has achieved high port isolation.

Table 4 compares the functional parameters of the developed MIMO antenna with those of the reported antenna. The table shows that the return loss (S_{11}), gain, isolation, and ECC are enhanced than the reported ones. Table 4 shows that our proposed scheme provides a better gain improvement. Above all, the proposed MIMO antenna provides a significant improvement in performance in all aspects. According to the comparison table, the proposed antenna outperforms the reported one. As a result, it could be integrated into real-time on-demand applications.

6. Conclusion

The proposed Yagi–Uda MIMO antenna is intended to outperform traditional MIMO antennas. In Microwave 13 Studio with CST, two prototype antennas are designed and then fabricated and tested for comparison. The size of the antenna is 120 mm × 70 mm. The proposed antenna has a return loss of −30 dB at 2.1 GHz and a loss of −44 dB at 2.5 GHz. At *S*-band, the antenna resonates at two frequencies. Furthermore, the two 1 × 4 element MIMO array antennas have a maximum gain of 12.1 dBi. For many radar applications, the suggested antenna is a strong competitor. MIMO cluster antenna with different dipole plans can accordingly be utilized for *S*-band broadband radar correspondence.

Data Availability

The data used to support the findings of this study are available from the corresponding author upon request.

Conflicts of Interest

The authors declare that they have no conflicts of interest.

References

[1] Y. Kou, X. Wang, C. Liu, and H. Gao, "Design of a UWB planar quasi Yagi-Uda antenna on S-C band," *IET International Radar Conference Hangzhou*, vol. 13, pp. 1–4, 2015.

[2] T. Maruyama, T. Uesaka, S. Yamaguchi, M. Ohtsuka, and H. Miyashita, "Four-element array antenna based on pattern reconfigurable Yagi-Uda antenna with complementary parasitic elements," in *Proceedings of the IEEE 4th Asia-Pacific Conference on Antennas and Propagation (APCAP)*, pp. 183-184, Bali, Indonesia, June 2015.

[3] J. Yeo, J. I. Lee, and J. T. Park, "Broadband series-fed dipole pair antenna with parasitic strip pair director," *Progress In Electromagnetics Research C*, vol. 45, pp. 1–13, 2013.

[4] C.-C. Yen and P. Nysen, "Broadband quasi-Yagi antenna with enhanced radiation pattern for MIMO applications," in *Proceedings of the IEEE Antennas and Propagation Society International Symposium (APSURSI)*, pp. 880-881, Orlando, FL, USA, July 2013.

[5] K. Malaisamy, M. Santhi, S. Robinson, M. Wasim, and P. Murugapandiyan, "Design and development of cross dipole antenna for satellite applications," *Frequenz*, vol. 74, no. 7-8, pp. 229–237, 2020.

[6] Z. Wani and D. Kumar, "Erratum for: a compact 4 × 4 MIMO antenna for UWB applications," *Microwave and Optical Technology Letters*, vol. 58, no. 9, p. 2285, 2016.

[7] S. Mohammad, A. Nezhad, H. R. Hassani, and A. Foudazi, "A dual-band WLAN/UWB printed wide slot antenna for mimo/diversity applications," *Microwave and Optical Technology Letters*, vol. 55, no. 3, pp. 461–465, 2013.

[8] S. Saxena, B. K. Kanaujia, S. Dwari, S. Kumar, and R. Tiwari, "A compact dual-polarized MIMO antenna with distinct diversity performance for UWB applications," *IEEE Antennas and Wireless Propagation Letters*, vol. 16, pp. 3096–3099, 2017.

[9] H. F. Huang and S. G. Xiao, "'Compact MIMO antenna for b," *Microwave and Optical Technology Letters*, vol. 58, no. 4, pp. 783–787, 2016.

[10] D. Roddy, *Satellite Communications*, Tata McGraw Hill, New Delhi, Fourth Edition, 2017.

[11] L. Liu, S. W. Cheung, and T. I. Yuk, "Compact MIMO antenna for portable UWB applications with band-notched characteristic," *IEEE Transactions on Antennas and Propagation*, vol. 63, no. 5, pp. 1917–1924, 2015.

[12] H. Nam Dao, M. Krairiksh, and D. Thanh Le, "A design of switched-beam Yagi-Uda antenna for wireless sensor networks," in *Proceedings of the International Conference on Advanced Technologies for Communications (ATC)*, pp. 393–396, Hanoi, Vietnam, October 2016.

[13] S. Hakimi, S. Kamal Abdul Rahim, M. Idzam Sabran, A. Nyangwarimam Obadiah, and H. Mohamed, "Compact MIMO antenna for indoor UWB applications," *Microwave and Optical Technology Letters*, vol. 58, no. 10, pp. 2387–2393, 2016.

[14] B. Honarbaksh, "High-gain low-cost microstrip antennas and arrays based on FR4 epoxy," *AUE-International Journal of Electronics and Communications*, vol. 75, pp. 1–7, 2017.

[15] M. Maqsood, S. Goa, T. W. C. Brown, M. Unwin, and R. De Vos Van Steenwijk, "Low-cost dual-band circularly polarized switched-beam array for global navigation satellite system," *IEEE Transactions on Antennas and Propagation*, vol. 62, no. 4, pp. 1975–1982, 2014.

[16] E. Fritz-Andrade, A. Perez-Miguel, R. Gomez-Villanueva, and H. Jardon-Aguilar, "Characteristic mode analysis applied to reduce the mutual coupling of a four-element patch MIMO antenna using a defected ground structure," *IET Microwaves, Antennas & Propagation*, vol. 14, no. 2, pp. 215–226, 2020.

[17] X. Zhao and S. Riaz, "A dual-band frequency reconfigurable MIMO patch-slot antenna based on reconfigurable microstrip feedline," *IEEE Access*, vol. 6, pp. 41450–41457, 2018.

[18] K. Malaisamy, M. Santhi, and S. Robinson, "Design and analysis of 4 × 4 MIMO antenna with DGS for WLAN applications," *International Journal of Microwave and Wireless Technologies*, vol. 13, pp. 979–985, 2021.

[19] S. Saxena, B. K. Kanaujia, S. Dwari, S. Kumar, H. C. Choi, and K. W. Kim, "Planar four-port dual circularly-polarized MIMO antenna for sub-6 GHz band," *IEEE Access*, vol. 8, pp. 90779–90791, 2020.

[20] K. R. Jha, Z. A. P. Jibran, C. Singh, and S. K. Sharma, "4-Port MIMO antenna using common radiator on a flexible substrate for sub-1GHz, sub-6GHz 5G NR, and wi-fi 6 applications," *IEEE Open Journal of Antennas and Propagation*, vol. 2, pp. 689–701, 2021.

[21] A. Ghalib and M. S. Sharawi, "TCM analysis of defected ground structures for MIMO antenna designs in mobile terminals," *IEEE Access*, vol. 5, pp. 19680–19692, 2017.

[22] S. F. Jilani and A. Alomainy, "Millimetre-wave T-shaped MIMO antenna with defected ground structures for 5G cellular networks," *IET Microwaves, Antennas & Propagation*, vol. 12, no. 5, pp. 672–677, 2018.

[23] Z. Tang, X. Wu, J. Zhan, S. Hu, Z. Xi, and Y. Liu, "Compact UWB-MIMO antenna with high isolation and triple band-notched characteristics," *IEEE Access*, vol. 7, pp. 19856–19865, 2019.

[24] S. Thummaluru and R. Chaudhary, "Mu-negative meta-material filter-based isolation technique for MIMO antennas," *Electronics Letters*, vol. 53, no. 10, pp. 644–646, 2017.

[25] J. Kulkarni, A. Desai, and C.-Y. Desmond Sim, "Wideband four-port MIMO antenna array with high isolation for future wireless systems," *AEU-International Journal of Electronics and Communications*, vol. 46, p. 145, 2020.

[26] N. P. Kulkarni, N. Bhaskarrao Bahadure, P. Patil, and J. S. Kulkarni, "Flexible interconnected 4-port MIMO antenna for sub-6 GHz 5G and X band applications," *AEU - International Journal of Electronics and Communications*, vol. 152, p. 154243, 2022.

[27] J. Kulkarni, C. YD. Sim, A. Desai et al., "A compact four port ground-coupled CPWG- fed MIMO antenna for wireless applications," *Arabian Journal for Science and Engineering*, vol. 47, no. 11, pp. 14087–14103, 2022.